ARL-TR-7584 ● JAN 2016

US Army Research Laboratory

Grain Boundary Engineering of Lithium-Ion-Conducting Lithium Lanthanum Titanate for Lithium-Air Batteries

by Victoria L Blair, Claire V Weiss Brennan, and Joseph M Marsico

NOTICES

Disclaimers

The findings in this report are not to be construed as an official Department of the Army position unless so designated by other authorized documents.

Citation of manufacturer's or trade names does not constitute an official endorsement or approval of the use thereof.

Destroy this report when it is no longer needed. Do not return it to the originator.

ARL-TR-7584 ● JAN 2016

US Army Research Laboratory

Grain Boundary Engineering of Lithium-Ion-Conducting Lithium Lanthanum Titanate for Lithium-Air Batteries

by Victoria L Blair and Claire V Weiss Brennan
Weapons and Materials Research Directorate, ARL

Joseph M Marsico
Rochester Institute of Technology, Rochester, NY

REPORT DOCUMENTATION PAGE

Form Approved
OMB No. 0704-0188

1. REPORT DATE *(DD-MM-YYYY)*	2. REPORT TYPE	3. DATES COVERED (From - To)
January 2016	Final	1–31 August 2014

4. TITLE AND SUBTITLE
Grain Boundary Engineering of Lithium-Ion-Conducting Lithium Lanthanum Titanate for Lithium-Air Batteries

5a. CONTRACT NUMBER

5b. GRANT NUMBER

5c. PROGRAM ELEMENT NUMBER

6. AUTHOR(S)
Victoria L Blair, Claire V Weiss Brennan, and Joseph M Marsico

5d. PROJECT NUMBER

5e. TASK NUMBER

5f. WORK UNIT NUMBER

7. PERFORMING ORGANIZATION NAME(S) AND ADDRESS(ES)
US Army Research Laboratory
ATTN: RDRL-WMM-E
Aberdeen Proving Ground, MD 21005-5069

8. PERFORMING ORGANIZATION REPORT NUMBER
ARL-TR-7584

9. SPONSORING/MONITORING AGENCY NAME(S) AND ADDRESS(ES)

10. SPONSOR/MONITOR'S ACRONYM(S)

11. SPONSOR/MONITOR'S REPORT NUMBER(S)

12. DISTRIBUTION/AVAILABILITY STATEMENT
Approved for public release; distribution is unlimited.

13. SUPPLEMENTARY NOTES

14. ABSTRACT
Soldiers currently have 6–8 h worth of batteries to power all of their personal communication devices, which is currently limiting the mission operational time. To improve the mission time, current technology could be replaced with lithium (Li)-air batteries, which have higher energy densities and a porous cathode. Li-air battery performance is limited by the electrolytic membrane, which needs high Li-ionic conductivity. Lithium lanthanum titanate ($Li_{3x}La_{(2/3)-x}TiO_3$, or LLTO) is a promising electrolytic membrane material due to its high lattice conductivity; however, the total conductivity of LLTO is lowered by its grain boundaries. We aim to increase the grain boundary conductivity by introducing an intergranular film (IGF) through novel processing techniques such as room temperature ion exchange and magnetron sputtering on a fluidized powder bed. After incorporation of the IGF, the grain boundary conductivity increased by up to 60% while maintaining crystal structure, microstructure, and density of the sintered pellets. The results of this study indicate that if the best-performing materials from this report are incorporated into a battery and all of the Soldier's batteries were replaced, the Soldier would be able to stay on-task in a mission for approximately 340 h without replacing batteries.

15. SUBJECT TERMS
ionic conductivity, ceramic processing, LLTO, intergranular film, grain boundary conductivity

16. SECURITY CLASSIFICATION OF:			17. LIMITATION OF ABSTRACT	18. NUMBER OF PAGES	19a. NAME OF RESPONSIBLE PERSON
a. REPORT	b. ABSTRACT	c. THIS PAGE			Victoria L Blair
Unclassified	Unclassified	Unclassified	UU	22	19b. TELEPHONE NUMBER (Include area code) 410-306-4947

Contents

List of Figures

List of Tables

Acknowledgments

Researchers at the US Army Research Laboratory's (ARL's) Weapons and Materials Research Directorate, Ceramics and Transparent Materials Branch, would like to thank Jeff Wolfenstine and Jan Allen (both at the Sensors and Electronic Devices Directorate) for their assistance in measuring the ionic conductivity of the samples, Dan Baechle for his assistance in the fluidized bed sputtering process, and ARL's Materials and Manufacturing Science Division for funding this 1-year seedling project.

INTENTIONALLY LEFT BLANK.

1. Introduction

Lithium (Li)-ion batteries are currently one of the leading energy storage device technologies and of interest to the US Army, which is developing novel battery materials to aid the Warfighter. The technologies employed (radios, surveillance equipment, etc.) by Soldiers require portable energy supplies, but current batteries can supply only 6–8 h of power to a Soldier's devices before they need to be replaced or charged. More devices could be powered for more than 72 h if novel battery devices are employed. Additionally, the number of batteries carried could be reduced if the energy density is higher, leading to a lower risk of Soldier musculoskeletal injuries. Li-air batteries have been the focus of recent research because they can store up to 10 times more energy than current batteries due to the porous "air" cathode, which also reduces the weight of the device.[1]

Both low-electrical and high-Li-ion conductivity are required for efficient battery operation, as chemical stability and mechanical robustness are needed for the reliability and safety of the battery, respectively. One of the most promising candidates for this membrane material is lithium lanthanum titanate ($Li_{3x}La_{(2/3)-x}TiO_3$, or LLTO) due to the material's high theoretical lattice conductivity.[2] In this report we will focus on LLTO with x = 0.11 ($Li_{0.33}La_{0.55}TiO_3$), as previous work indicates that LLTO ceramics with this composition exhibit the maximum lattice conductivity.[3,4] However, the total conductivity is dominated by low grain boundary conductivity. This study will focus on methods to improve the grain boundary conductivity by grain boundary engineering methods while maximizing the lattice conductivity through quenching from high temperature.

LLTO, a perovskite, comes in 2 different polymorphs: 1) tetragonal, P4/mmm, and 2) cubic, Pm3-m. The tetragonal structure is stabilized upon slow cooling from the sintering temperature of 1,200 °C. If a rapid cooling regime is used, such as quenching from the sintering temperature into liquid nitrogen (LN_2), the cubic phase (Pm-3m) is stabilized.[5–8] Harada et al.[5] were able to determine that LLTO is not just one polymorph; instead, it tends to crystallize with a ratio of both phases depending on the cooling schedule and the A-site composition. Additionally, Harada et al. show that the lattice conductivities (σ_l) for the tetragonal phase are 60% lower than that of the cubic phase. The change in lattice conductivity from one phase to the next may be due to the symmetry of the cubic space group. In the cubic phase, the angle between the octahedra (Fig. 1) is slightly larger than the angle in the tetragonal phase. This tilting of the octahedra could lead to a lower activation energy for Li-ion conduction through the cubic lattice, thus leading to a higher lattice conductivity.[5–8]

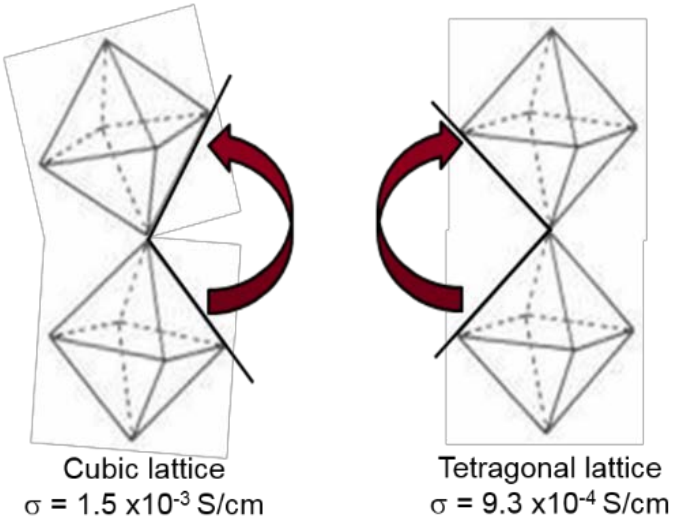

Fig. 1 Idealized cubic lattice (left) shows tilting of the octahedral, which causes a larger space for Li-ion conduction compared with the idealized tetragonal structure (right)

The low total conductivity observed in LLTO ceramic materials is thought to arise from 3 main factors: lithium deficiency, low density, and high-resistivity grain boundaries. All 3 of those factors influence each other; for example, sintering at higher temperatures might increase the density (thus increasing conductivity) but might also lead to Li loss through volatilization of lithium oxide and simultaneously decreasing conductivity due to loss of the main charge carriers.[2]

Recently there has been significant effort toward improving the grain boundary conductivity in LLTO and related ceramic membrane materials. One method to increase the grain boundary conductivity is to increase the density of the ceramic, approaching the theoretical density, as explored in Weiss Brennan et al.[9] Density optimization is expected to enhance grain boundary conductivity since recent transmission electron microscopy (TEM) results on LLTO indicate that a majority of the porosity exists at the grain boundaries.[10]

Increased surface area at the grain boundaries by improved density should enhance the Li-ion diffusion pathways at the grain boundaries; the minimization of the detrimental grain boundary second phase (air) should increase the total conductivity as well.[3,10] These ideas were partially explored in Weiss Brennan et. al.[9] The current study will examine different methods to improve the grain boundary conductivity through incorporation of intergranular films while maintaining the high density obtained in the previous study.[9] Current literature has examined several techniques, although only a few of them have been applied to LLTO.[10–12]

2. Experimental Work

2.1 Ceramic Processing

The LLTO powder was synthesized by the same method described in Weiss Brennan et al.,[9] a solid-state reaction method. After the calcination step, the powder was separated: a portion each for sputter coating with silicon dioxide (SiO_2), baseline pellets, and sintered pellets to be soaked in lithium chloride (LiCl). Table 1 outlines all of the experimental sample conditions for this report and the corresponding sample labels, which will be used to refer to the processing conditions.

Table 1 Sample labels and experimental conditions for this report

Cooling	Baseline, no treatment	SiO_2 sputtered coating	Li-ion stuffed
Standard	LLTO-BT	LLTO-ST	LLTO-LT
Rapid	LLTO-BC	LLTO-SC	LLTO-LC

Notes: SiO_2 = silicon dioxide; L = Li-ion; B = baseline; T = tetragonal; C = cubic; S = sputtered.

To sputter coat the calcined powder, the powder was placed into a sample cup installed in a vacuum chamber and vibrated to fluidize the powder bed. A magnetron sputter source with an SiO_2 target was turned on and remained on for a maximum of 8 h. Figure 2 shows the general schematic of the system as reported by Baechle et al.[13]

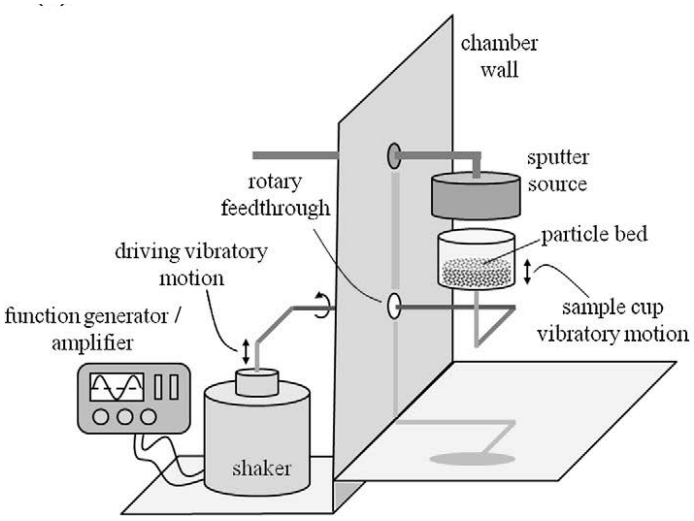

Fig. 2 General schematic of the fluidized bed setup for the magnetron sputtering completed in this report

The calcined and treated powders were uniaxially pressed into pellets at 5,000 psig in a 13-mm die. The pressed pellets were then vacuum sealed into plastic bags and cold isostatically pressed at 30,000 psig for 30 s. The pressed pellets were placed in closed alumina crucibles containing a sacrificial powder bed of the same composition. The powder bed was used to provide a Li-rich local environment around the pellets during sintering, which compensates for the Li vaporization that occurs above approximately 800 °C.[14]

The pellets in powder bed were sintered at 1,200 °C using a box furnace. The sintering process included a ramp rate of 10˚C/min up to 1,200 °C for 6 h and cooled to room temperature at the same rate. Following the sintering procedure, the pellets were ground down to remove any residual powder bed using silicon carbide (SiC) sandpaper. The pellets were then rinsed using deionized water and left in an oven to ensure complete water evaporation. Half of the pellets underwent an annealing cycle for 1 h at 1,200 °C and were quenched from high temperature into LN_2 to lock in the cubic LLTO polymorph.

To exchange the ceramic with free Li ions, sintered and quenched LLTO pellets (both tetragonal and cubic phase) were submerged in concentrated LiCl solution. The LiCl solution was made by dissolving lithium carbonate ($LiCO_3$) into hydrogen chloride until the pH reached approximately 7 and $LiCO_3$ began to settle on the bottom of the beaker. The solution was filtered to remove the undissolved powder before the pellets were submerged. The beaker was covered and left in a fume hood at room temperature for 7 days with the pellets completely covered by the LiCl solution.

2.2 Characterization Methods

The apparent and bulk densities were measured using 2 variations of the Archimedes method with a Mettler Toledo AX205 balance as described in Sutorik et al.[2] The bulk density is a measure of the open porosity. Therefore, the use of both Archimedes density calculations provides information not only on the ceramic density, but also on the closed versus open porosity for each sample. For example, if the bulk density and the apparent density are the same, the sample contains no open porosity—only closed porosity.

X-ray diffraction (XRD) patterns and analysis were conducted on the sintered samples to determine crystallographic and phase information of the ceramic pellets. XRD patterns were collected on a Rigaku MiniFlex II using copper Kα radiation. A Hitachi 4700 scanning electron microscope (SEM) was used to observe the sintered microstructures of the ceramic pellets typically using an accelerating

voltage of 2–5 kV. The samples were polished using diamond suspension down to 0.25 µm and thermally etched at 1,100 °C for 1 h.

To measure the ionic conductivity of the LLTO pellets, the top and bottom faces of the pellets were polished with SiC paper before being sputter coated with platinum or gold. Electrical conductivity measurements were performed on the metal-coated samples using the 2-probe method. Room temperature Li-ion conductivity was determined from alternating-current electrochemical impedance spectroscopy using a Bio-logic SP200 over a frequency range of 0.1 Hz–7 MHz with a potential amplitude of 100 mV. The bulk, grain boundary, and electrode contributions to the impedance spectra were separated by fitting the spectra using ZView (Scribner Associates, Inc.).[15]

3. Results and Discussion

After sintering, the densities of the pellets sintered at 1,200 °C achieved greater than 95% of the theoretical density (~5.05 g/cm^3) for tetragonal LLTO. For all pellets, the bulk and apparent densities were similar, indicating little open porosity remains in the pellet. The SEM micrographs for all pellets were also similar, with grains approximately 3 µm in size. Figure 3 shows 2 images, one from the untreated LLTO (LLTO-BT) and one from SiO_2-coated LLTO (LLTO-ST). The coated sample appears to have a hairy, fiber-like coating. Energy-dispersive X-ray spectroscopy results indicate that Si is indeed in the bulk of the coated sample and not in the untreated sample. Future TEM results will confirm the location of the Si at the grain boundary and show any differences in the grain boundaries from the baseline to the coated samples.

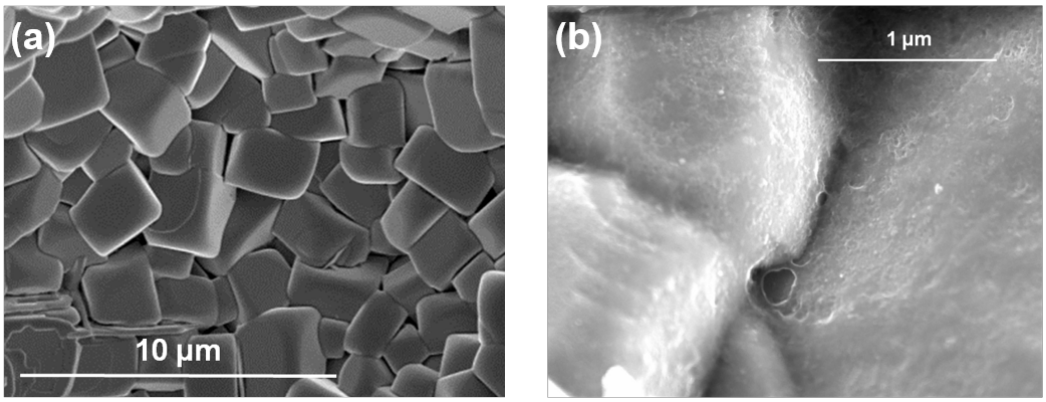

Fig. 3 SEM micrographs of a) LLTO-BT and b) LLTO-ST, the latter showing a thin, hairy coating that could be the SiO_2 sputtered onto the grains before densification. LLTO-BT does not have a hairy coating.

XRD revealed that the pellets were mainly tetragonal-phase LLTO, given by the space group P4/mmm if cooled slowly from high temperature. If the pellet was quenched from high temperature into LN_2, the space group was Pm3-m. Table 2 shows the lattice and grain boundary conductivities for all the specimens discussed in this report.

Table 2 Experimental conditions, sample labels, and ionic conductivity results

	Baseline, no treatment (LLTO-B)	**SiO_2 sputtered coating (LLTO-S)**	**Li-ion stuffed (LLTO-L)**
>80% tetragonal structure (T)	**LLTO-BT** $\sigma_l = 9.3 \times 10^{-4}$ S/cm $\sigma_{gb} = 2.5 \times 10^{-5}$ S/cm	**LLTO-ST** $\sigma_l = 9.5 \times 10^{-4}$ S/cm $\sigma_{gb} = 3.3 \times 10^{-5}$ S/cm	**LLTO-LT** $\sigma_l = 9.0 \times 10^{-4}$ S/cm $\sigma_{gb} = 4.2 \times 10^{-5}$ S/cm
>80% cubic structure (C)	**LLTO-BC** $\sigma_l = 1.5 \times 10^{-3}$ S/cm $\sigma_{gb} = 7.2 \times 10^{-6}$ S/cm	**LLTO-SC** $\sigma_l = 1.1 \times 10^{-3}$ S/cm $\sigma_{gb} = 7.1 \times 10^{-5}$ S/cm	**LLTO-LC** $\sigma_l = 1.0 \times 10^{-3}$ S/cm $\sigma_{gb} = 1.2 \times 10^{-5}$ S/cm

LLTO samples that were sputter coated (LLTO-ST and LLTO-SC) showed interesting conductivity results, plotted in Figs. 4 and 5. Any bar above the red line indicates an improvement over the baseline samples (LLTO-BT and LLTO-BC).

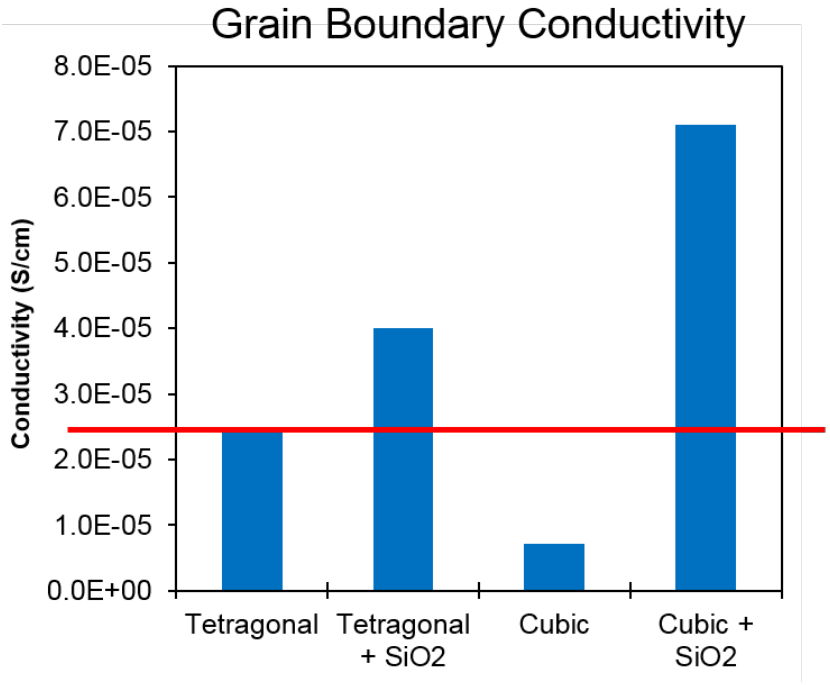

Fig. 4 Grain boundary conductivity for the SiO_2-coated samples (LLTO-ST and LLTO-SC) and the control samples (LLTO-BT and LLTO-BC); red line indicates the baseline LLTO conductivity value

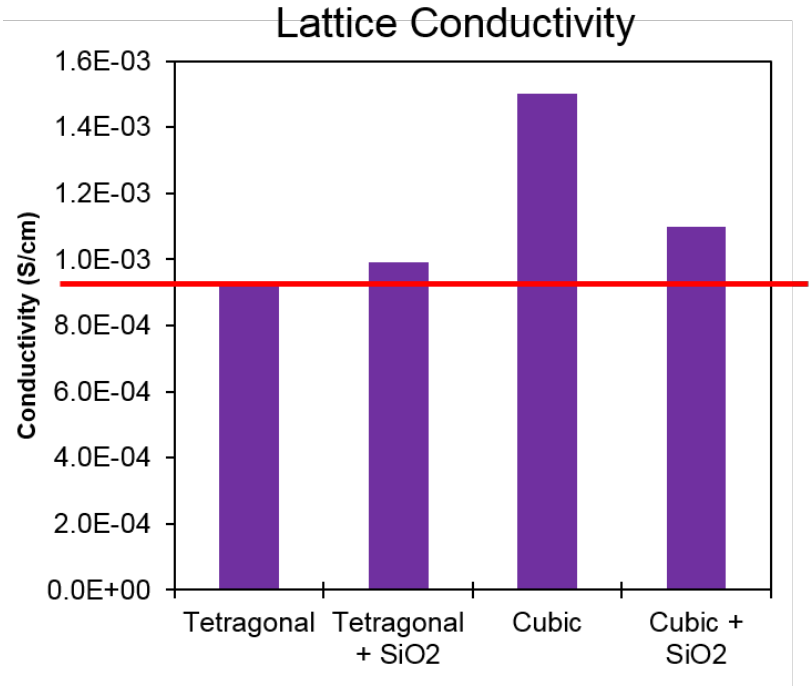

Fig. 5 Lattice conductivity for the SiO_2-coated samples (LLTO-ST and LLTO-SC) and the control samples (LLTO-BT and LLTO-BC); red line indicates the baseline LLTO conductivity value

The SiO_2 samples have higher grain boundary conductivity than the baseline (LLTO-ST and LLTO-SC). This indicates that the fluidized bed and sputter coating method is essential in increasing the grain boundary conductivity. In addition, the SiO_2 coating method does not appear to have a negative effect on the lattice conductivity. However, forcing the cubic lattice onto LLTO-BC leads to a lower grain boundary conductivity. This could be a result of the second sintering cycle to quench from 1,200 °C. There was a risk of losing more Li ions from the material, and therefore some charge carriers were lost. Also, there is research suggesting the Li tends to leave the grain boundaries first, which also can be confirmed with detailed TEM analysis.[16–18]

The Li-ion-rich samples show no major differences in microstructure or phase composition according to SEM and XRD, respectively. However, the conductivity results were different from the SiO_2-coated samples, as shown in Figs. 6 and 7.

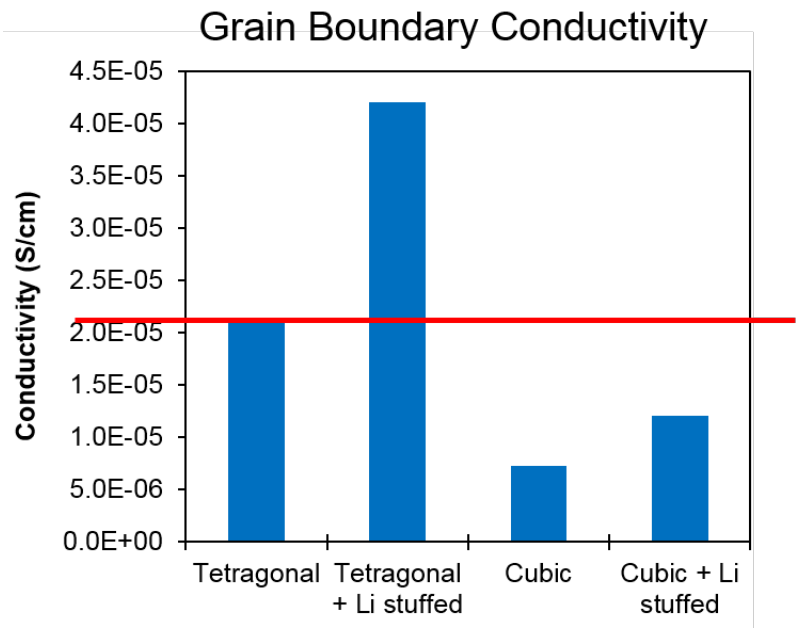

Fig. 6 Grain boundary conductivity for the LiCl-soaked samples (LLTO-LT and LLTO-LC) and the control samples (LLTO-BT and LLTO-BC); red line indicates the baseline LLTO conductivity value

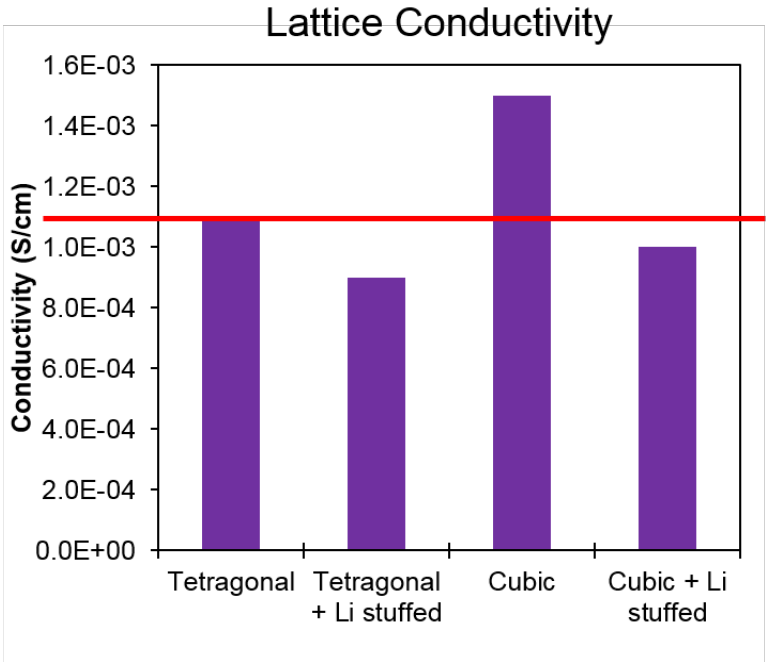

Fig. 7 Lattice conductivity for the LiCl-soaked samples (LLTO-LT and LLTO-LC) and the control samples (LLTO-BT and LLTO-BC); red line indicates the baseline LLTO conductivity value

The grain boundary for the tetragonal and Li-rich sample (LLTO-LT) is increased by a factor of 2. The excess Li in the LiCl solution went to the Li-deficient areas of the pellet, which have been known to be the grain boundaries.[3,19] The increase in the concentration of charge carries led to an increase in the grain boundary conductivity. However, the Li-rich sample in the cubic phase (LLTO-LC) appears to have a lower grain boundary conductivity. It is possible that this particular sample has too many charge carriers, which could suppress the conductivity.

There is likely an ideal ratio of Li ions and A-site vacancies for the Li-ions to travel through to get a maximum in the conductivity. Kawai and Kuwano[4] indicate that there is an Li concentration, x = 0.11 in $Li_{3x}La_{(2/3)-x}TiO_3$, at which the ionic conductivity is a maximum, which has been studied previously. That particular composition is what this study used for all the base LLTO powders. However, the Li concentration likely changed during processing, as mentioned earlier. Future inductively coupled plasma mass spectrometry (ICP-MS) studies will confirm the total Li content and could show the trend in conductivity with Li concentration to guide new research as well as optimize the Li exchange process. The added Li in the lattice might be taking away the vacancies for charge carries to travel through, thus lowering the lattice conductivity. This was also reported in Kawai and Kuwano.[4]

Using a "back of the envelope" calculation, if the highest performing material was incorporated into a battery, the total battery lifetime will be increased so much that a Soldier's on-task mission time can be extended to 340 h. This value was calculated by assuming that Soldiers run out of battery power after 8 h of use and all 20 lb of batteries (carried by a Soldier) are replaced by Li-air batteries using our particular material with an approximately 3× improvement over the current standard.

4. Summary and Conclusions

Several processing conditions for LLTO were examined including structure control (tetragonal LLTO vs. cubic LLTO), adding an SiO_2 layer by sputtering onto a fluidized powder bed, and Li-ion exchange by soaking in a concentrated LiCl solution. All methods increased the conductivity to some extent. The grain boundary conductivity improved by up to 60% when a thin layer of SiO_2 was sputtered onto the surface of LLTO powder before densification. Lattice conductivity was improved in LLTO by quenching the samples into LN_2 from high temperatures to stabilize the cubic structure. Combining both the cubic structure with an SiO_2 coating led to an increase in both conductivity contributions; grain

boundary conductivity improved by a factor of approximately 3. Stuffing the lattice and grain boundaries with Li ions from LiCl increases the grain boundary contribution by 60% but at the cost of the lattice conductivity. All results indicate that the concentration of Li with respect to available vacancies is important to the conductivity of the overall material.

Future work should confirm the concentration of Li in the material along with TEM to evaluate if an intergranular film was achieved by the magnetron-sputtering method. Electron energy loss spectroscopy should also be conducted to determine if there is a variation in the Li concentration at the grain boundaries. ICP-MS could give the bulk amount of Li in the ceramic material that may be correlated to the ionic conductivity data. Barring the other engineering challenges, the advancements described in this report on processing LLTO could lead to a major improvement in battery life during fielded Soldier missions.

5. References

1. Padbury R, Zhang X. Lithium-oxygen batteries: limiting factors that affect performance. Journal of Power Sources. 2011;196:4436–4444.

2. Sutorik A, Green M, Cooper C, Wolfenstine J, Gilde G. The comparative influences of structural ordering, grain size, Li-content, and bulk density on the Li^+-conductivity of $Li_{0.29}La_{0.57}TiO_3$. J Mater Sci. 2012;47:6992–7002.

3. Stramare S, Thangadurai V, Weppner W. Lithium lanthanum titanates: a review. Chemistry of Materials. 2003;15:3974–3990.

4. Kawai H, Kuwano J. Lithium ion conductivity of A-site deficient perovskite solid solution $La_{0.67-x}Li_{3x}TiO_3$. Journal of the Electrochemical Society. 1994;141:L78.

5. Harada Y, Hirakoso Y, Kawai H, Kuwano J. Order–disorder of the A-site ions and lithium ion conductivity in the perovskite solid solution $La_{0.67-x}Li_{3x}TiO_3$ (x=0.11). Journal of Solid State Ionics. 1999;121:245–251.

6. Inaguma Y, Katsumata T, Itoh M, Morii Y. Crystal structure of a lithium ion-conducting perovskite $La_{2/3-x}Li_{3x}TiO_3$ (x=0.05). Journal of Solid State Chemistry. 2002;166:67–72.

7. Sommariva M, Catti M. Neutron diffraction study of quenched $Li_{0.3}La_{0.567}TiO_3$ lithium ion conducting perovskite. Chemistry of Materials. 2006;18:2411–2417.

8. Varez A, Fernández-Díaz MT, Alonso JA, Sanz J. Structure of fast ion conductors $Li_{3x}La_{2/3-x}TiO_3$ deduced from powder neutron diffraction experiments. Chemistry of Materials. 2005;17:2404–2412.

9. Weiss Brennan CV, Blair VL, Marsico JM. Density optimization of lithium lanthanum titanate ceramics for lightweight lithium-air batteries. Aberdeen Proving Ground (MD): Army Research Laboratory (US); 2014 Dec. Report No.: ARL-TR-7145.

10. Ban CW, Choi GM. The effect of sintering on the grain boundary conductivity of lithium lanthanum titanates. Solid State Ionics. 2001;140:285–292.

11. Kim KH, Hirayama T, Fisher CAJ, Yamamoto K, Sato T, Tanabe K, Kumazaki S, Iriyama Y, Ogumi Z. Characterization of grain-boundary phases in $Li_7La_3Zr_2O_{12}$ solid electrolytes. Materials Characterization. 2014;91:101–106.

12. Mei A, Wang X-L, Lan J-L, Feng Y-C, Geng H-X, Lin Y-H, Nan C-W. Role of amorphous boundary layer in enhancing ionic conductivity of lithium-lanthanum-titanate electrolyte. Electrochimica Acta. 2010;55:2958–2963.

13. Baechle DM, Demaree JD, Hirvonen JK, Wetzel ED. Magnetron sputter deposition onto fluidized particle beds. Surface and Coatings Technology. 2013;221:94–103.

14. Inada R, Kimura K, Kusakabe K, Tojo T, Sakurai Y. Synthesis and lithium-ion conductivity for perovskite-type $Li_{3/8}Sr_{7/16}Ta_{3/4}Zr_{1/4}O_3$ solid electrolyte by powder-bed sintering. Solid State Ionics. 2014;261: 95–99.

15. Wolfenstine J, Allen J, Weiss Brennan CV, Blair VL. Conductivity of hot isostatically pressed $Li_{0.35}La_{0.55}TiO_3$. Aberdeen Proving Ground (MD): Army Research Laboratory (US); 2015 Aug. Report No.: ARL-TR-7401.

16. Cao W, Kundu A, Yu Z, Harmer MP, Vinci RP. Direct correlations between fracture toughness and grain boundary segregation behavior in ytterbium-doped magnesium aluminate spinel. Scripta Materialia. 2013;69:81–84.

17. Gao X, Fisher CAJ, Kimura T, Ikuhara YH, Kuwabara A, Moriwake H, Oki H, Tojigamori T, Kohama K, Ikuhara Y. Domain boundary structures in lanthanum lithium titanates. Journal of Materials Chemistry A. 2014;2:843–852.

18. Ma C, Chen K, Liang C, Nan C-W, Ishikawa R, More K, Chi M. Atomic-scale origin of the large grain-boundary resistance in perovskite Li-ion-conducting solid electrolytes. Energy and Environmental Science. 2014;7:1638–1642.

19. Knauth P. Inorganic solid Li ion conductors: an overview. Solid State Ionics. 2009;180(14–16):911–916.

List of Symbols, Abbreviations, and Acronyms

σ_l	lattice conductivities
ICP-MS	inductively coupled plasma mass spectrometry
Li	lithium
$Li_{3x}La_{(2/3)-x}TiO_3$	lithium lanthanum titanate
LiCl	lithium chloride
$LiCO_3$	lithium carbonate
LLTO	lithium lanthanum titanate
LN_2	liquid nitrogen
SEM	scanning electron microscope
SiC	silicon carbide
SiO_2	silicon dioxide
TEM	transmission electron microscopy
XRD	X-ray diffraction

1 (PDF) DEFENSE TECHNICAL INFORMATION CTR DTIC OCA

2 (PDF) DIRECTOR US ARMY RESEARCH LAB RDRL CIO LL IMAL HRA MAIL & RECORDS MGMT

1 (PDF) GOVT PRINTG OFC A MALHOTRA

1 (PDF) DIR USARL RDRL WMM E VL BLAIR